JOC Article

Azolium-Linked Cyclophanes: Effects of Structure, Solvent, and Counteranions on Solution Conformation Behavior

Murray V. Baker,*[,†] David H. Brown,[†,‡] Charles H. Heath,[†] Brian W. Skelton,[†] Allan H. White,[†] and Charlotte C. Williams[†]

Chemistry M313, School of Biomedical, Biomolecular and Chemical Sciences, The University of Western Australia, Crawley, WA 6009, Australia, and Nanochemistry Research Institute, Department of Applied Chemistry, Curtin University of Technology, GPO Box U1987, Perth WA 6845, Australia

murray.baker@uwa.edu.au

Received August 21, 2008

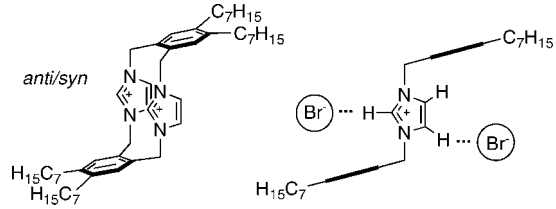

This paper describes the synthesis, structural characterization, and solution behavior of some xylyl-linked imidazolium and benzimidazolium cyclophanes decorated with alkyl or alkoxy groups. The addition of alkyl/alkoxy chains to the cyclophanes allows for studies in chlorinated solvents, whereas previous solution studies of azolium cyclophanes have generally required highly polar solvents. The azolium cyclophanes may exist in a *syn*/*syn* conformation (azolium rings mutually *syn*, arene rings mutually *syn*) or a *syn*/*anti* conformation (azolium rings mutually *syn*, arene rings mutually *anti*). The preferred conformation is significantly affected by (i) binding of bromide (ion pairing) to the protons on the imidazolium or benzimidazolium rings, which occurs in solutions of bromide salts of the cyclophanes in chlorinated solvents, and (ii) the addition of alkoxy groups to the benzimidazolium cyclophanes. These structural modifications have also led to cyclophanes that adopt conformations not previously identified for similar azolium cyclophane analogues. Detailed ^{1}H NMR studies for one cyclophane identified binding of bromide at two independent sites within the cyclophane.

Introduction

Over the past decade, azolium cyclophanes have been of significant interest.[1] Studies involving this class of cyclophanes have focused on challenges associated with synthesis, their intriguing conformational behavior, and, in particular, their potential applications in anion recognition and, in the case of imidazolium- and benzimidazolium-based cyclophanes, the use of them as precursors to N-heterocyclic carbene metal complexes.

Anion binding involving imidazolium cyclophanes is primarily based on hydrogen bonding of the anion with the acidic H2 proton of the imidazolium cation.[2−6] Design of specific imidazolium cyclophane structures has led to cyclophanes that display improved binding to specific anions; for example, **1**[4] and **2**[5] bind dihydrogenphosphate and fluoride preferentially, respectively.

We have been interested in azolium cyclophanes containing imidazolium or benzimidazolium moieties linked by xylyl groups, for example, cyclophanes **3**−**5**.[7] These types of cyclophanes can exhibit fluxional behavior in solution involving the

[†] The University of Western Australia.
[‡] Curtin University of Technology.

(1) For a review, see: Baker, M. V.; Brown, D. H. *Mini-Rev. Org. Chem.* **2006**, *3*, 333–354.

(2) Alcalde, E.; Alvarez-Rúa, C.; García-Granda, S.; García-Rodriguez, E.; Mesquida, N.; Pérez-García, L. *Chem. Commun.* **1999**, 295–296.

(3) (a) Yuan, Y.; Gao, G.; Jiang, Z.-L.; You, J.-S.; Zhou, Z.-Y.; Yuan, D.-Q.; Xie, R.-G. *Tetrahedron* **2002**, *58*, 8993–8999. (b) Yoon, J.; Kim, S. K.; Singh, N. J.; Kim, K. S. *Chem. Soc. Rev.* **2006**, *35*, 355–360. (c) Singh, N. J.; Jun, E. J.; Chellappan, K.; Thangadurai, D.; Chandran, R. P.; Hwang, I.-C.; Yoon, J.; Kim, K. S. *Org. Lett.* **2007**, *9*, 485–488. (d) Niu, H.-T.; Yin, Z.; Su, D.; Niu, D.; Ao, Y.; He, J.; Cheng, J.-P. *Tetrahedron* **2008**, *64*, 6300–6306.

(4) Yoon, J.; Kim, S. K.; Singh, N. J.; Lee, J. W.; Yang, Y. J.; Chellappan, K.; Kim, K. S. *J. Org. Chem.* **2004**, *69*, 581–583.

(5) Chellappan, K.; Singh, N. J.; Hwang, I.-C.; Lee, J. W.; Kim, K. S. *Angew. Chem., Int. Ed.* **2005**, *44*, 2899–2903.

(6) Alcalde, E.; Mesquida, N.; Pérez-García, L. *Eur. J. Org. Chem.* **2006**, 3988–3996.

(7) Baker, M. V.; Bosnich, M. J.; Brown, D. H.; Byrne, L. T.; Hesler, V. J.; Skelton, B. W.; White, A. H.; Williams, C. C. *J. Org. Chem.* **2004**, *69*, 7640–7652.

10.1021/jo801860d CCC: $40.75 © 2008 American Chemical Society
Published on Web 11/05/2008

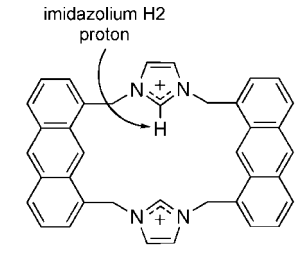

1

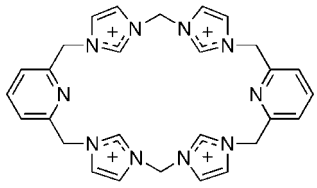

2

interconversion of different conformers.[7,8] In some cases, during low-temperature NMR studies, the fluxional behavior can be "frozen-out" and the different conformers identified based on their signals in the ^{1}H NMR spectra. In general, azolium cyclophanes such as **3**−**5** exhibit very low solubility in nonpolar organic solvents, so the VT-NMR studies have been restricted to solutions of the cyclophanes in highly polar solvents such as DMSO and methanol.

Our interest in these salts is primarily based on their ability to act as precursors to N-heterocyclic carbenes (NHCs) which can form a range of metal complexes. For instance, we and others have reported the synthesis and characterization of Pd(II) (e.g., **6**), Ni(II), Pt(II), Rh(I), Ir(I), Au(I) (e.g., **7**), and Ag(I) complexes with NHCs derived from azolium cyclophanes.[9−16] The properties of these complexes are varied and include catalytic behavior of Pd(II) complexes in Heck and Suzuki reactions,[10,11,15] Au(I) complexes that are luminescent and exhibit potential antimitochondrial antitumor behavior,[14,17] and Ag(I) complexes that display antimicrobial activity.[13,18] Complexes such as **6** and **7** tend to exhibit low solubility in organic solvents, paralleling the low solubility of the precursor azolium cyclophane **3**. We have attempted to improve the solubility of the metal complexes in organic solvents by substitution of the cyclophane skeleton with extended alkyl chains, and so have explored the synthesis and properties of imidazolium cyclophane salts such as **8**−**10**.[10,12,15] These cyclophanes (**8**−**10**) exhibit remarkably different solubilities compared to the cyclophanes **3**−**5**, readily dissolving in chlorinated solvents such as chloroform and dichloromethane. The cyclophanes also exhibit significantly different solution behavior in chlorinated solvents compared to DMSO and methanol, as identified in ^{1}H NMR spectroscopy studies. This behavior appears to be a consequence of halide interactions with the acidic imidazolium H2 protons of the cyclophanes.

In this paper, we discuss the conformational behavior of cyclophanes bearing extended alkyl chains. Our aim here is to (i) understand the conformational behavior of the new alkyl-substituted cyclophanes compared to the previously studied systems; (ii) explore the effect of solvent on conformation; and (iii) explore the effect of counteranions on the solution behavior of the cyclophanes.

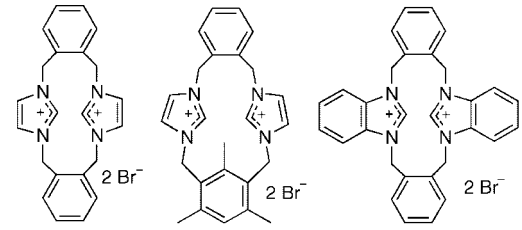

3.2Br **4**.2Br **5**.2Br

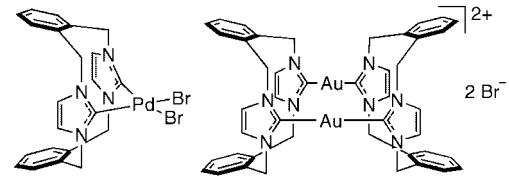

6 **7**

The discussion in this paper is assisted by a brief summary of the solution behavior of the previously studied cyclophane salts **3**·2Br−**5**·2Br.[7,19] The variable-temperature ^{1}H NMR studies were performed using DMSO-d_6 or CD_3OD solutions. The range of solvents was limited because of the low solubility of these salts in organic solvents. The room-temperature ^{1}H NMR spectra of **3**·2Br exhibited very broad signals for the benzylic and imidazolium protons, the broad signals indicating the probable occurrence of exchange processes. In DMSO-d_6, the H2 imidazolium proton is observed; however, in CD_3OD, the imidazolium H2 proton undergoes rapid H/D exchange and is not observed.[7] At low temperature, the exchange processes were sufficiently slow that sharp ^{1}H NMR signals were detected for two different conformers, the structures of which were determined from the chemical shifts of the signals in the ^{1}H NMR spectrum. In both conformers, the imidazolium rings were mutually *syn*, but the benzene rings were *anti* in one conformer and *syn* in the other (Scheme 1). Two different dynamic processes were identified: rotation of the imidazolium rings about their N−N axis, which interconverted the two different

(8) Bitter, I.; Török, Z.; Csokai, V.; Grün, A.; Balázs, B.; Tóth, G.; Keserü, G. M.; Kovári, Z.; Czugler, M. *Eur. J. Org. Chem.* **2001**, 2861–2868.

(9) (a) Shi, Z.; Thummel, R. P. *Tetrahedron Lett.* **1995**, *36*, 2741–2744. (b) Garrison, J. C.; Simons, R. S.; Kofron, W. G.; Tessier, C. A.; Youngs, W. J. *Chem. Commun.* **2001**, 1780–1781. (c) Garrison, J. C.; Simons, R. S.; Talley, J. M.; Wesdemiotis, C.; Tessier, C. A.; Youngs, W. J. *Organometallics* **2001**, *20*, 1276–1278. (d) Baker, M. V.; Skelton, B. W.; White, A. H.; Williams, C. C. *Organometallics* **2002**, *21*, 2674–2678. (e) Garrison, J. C.; Simons, R. S.; Tessier, C. A.; Youngs, W. J. *J. Organomet. Chem.* **2003**, *673*, 1–4. (f) Barnard, P. J.; Baker, M. V.; Berners-Price, S. J.; Skelton, B. W.; White, A. H. *Dalton Trans.* **2004**, 1038–1047. (g) Baker, M. V.; Brayshaw, S. K.; Skelton, B. W.; White, A. H.; Williams, C. C. *J. Organomet. Chem.* **2005**, *690*, 2312–2322.

(10) Baker, M. V.; Skelton, B. W.; White, A. H.; Williams, C. C. *J. Chem. Soc., Dalton Trans.* **2001**, 111–120.

(11) Magill, A. M.; McGuinness, D. S.; Cavell, K. J.; Britovsek, G. J. P.; Gibson, V. C.; White, A. J. P.; Williams, D. J.; White, A. H.; Skelton, B. W. *J. Organomet. Chem.* **2001**, *617*−*618*, 546–560.

(12) Baker, M. V.; Brown, D. H.; Haque, R. A.; Skelton, B. W.; White, A. H. *Dalton Trans.* **2004**, 3756–3764.

(13) Melaiye, A.; Sun, Z.; Hindi, K.; Milsted, A.; Ely, D.; Renekerm, D. H.; Tessier, C. A.; Youngs, W. J. *J. Am. Chem. Soc.* **2005**, *127*, 2285–2291.

(14) Barnard, P. J.; Wedlock, L. E.; Baker, M. V.; Berners-Price, S. J.; Joyce, D. A.; Skelton, B. W.; Steer, J. H. *Angew. Chem., Int. Ed.* **2006**, 5966–5970.

(15) Baker, M. V.; Brown, D. H.; Simpson, P. V.; Skelton, B. W.; White, A. H.; Williams, C. C. *J. Organomet. Chem.* **2006**, *691*, 5845–5855.

(16) Baker, M. V.; Brown, D. H.; Hesler, V. J.; Skelton, B. W.; White, A. H. *Organometallics* **2007**, *26*, 250–252.

(17) Barnard, P. J.; Baker, M. V.; Berners-Price, S. J.; Day, D. A. *J. Inorg. Biochem.* **2004**, *98*, 1642–1647.

(18) Kascatan-Nebioglu, A.; Panzner, M. J.; Tessier, C. A.; Cannon, C. L.; Youngs, W. J. *Coord. Chem. Rev.* **2007**, *251*, 884–895.

(19) Shi, Z.; Thummel, R. P. *J. Org. Chem.* **1995**, *60*, 5935–5945.

SCHEME 1. Interconversion of the *anti* and *syn* Conformers of 3

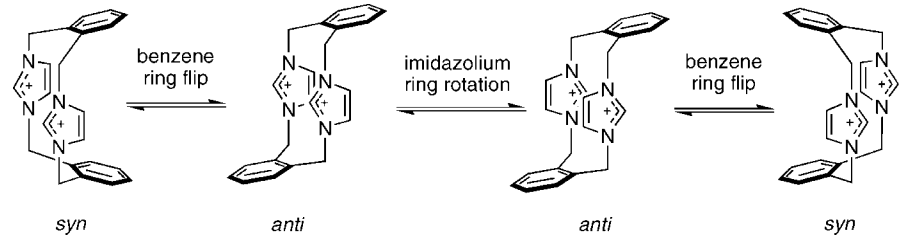

TABLE 1. Rate Constant and Free Energy of Activation for the Exchange Processes of the Cyclophanes 3, 5, and 8

cyclophane	anion	solvent	*anti*:*syn*[a]	k (*anti*→*anti*[b])	$\Delta G^{\ddagger}$ (*anti*→*anti*)	k (*anti*→*syn*[b])	$\Delta G^{\ddagger}$ (*anti*→*syn*)
3[c]	Br	CD_3OD	0.78:0.22	740 s^{-1} @ −13 °C	49 kJ mol^{-1}	120 s^{-1} @ 27 °C	61 kJ mol^{-1}
8	Br	CD_3OD	0.74:0.26	775 s^{-1} @ −20 °C	48 kJ mol^{-1}	160 s^{-1} @ 20 °C	59 kJ mol^{-1}
8	Br	CD_2Cl_2	1:0	104 s^{-1} @ 5 °C	57 kJ mol^{-1}	*d*	*d*
8	PF_6	CD_3OD	0.81:0.19	677 s^{-1} @ −20 °C	47 kJ mol^{-1}	107 s^{-1} @ 20 °C	60 kJ mol^{-1}
8	PF_6	CD_2Cl_2	0.85:0.15	82 s^{-1} @ −15 °C	53 kJ mol^{-1}	84 s^{-1} @ 25 °C	61 kJ mol^{-1}
5[e]	Br	DMSO-d_6					61 kJ mol^{-1}

[a] Population ratio at low exchange limit (low temp). [b] Processes: *anti*→*anti* imidazolium ring rotation; *anti*→*syn* arene ring flip. [c] Ref 7. [d] Could not be determined. Coalescence not reached. [e] Ref 19.

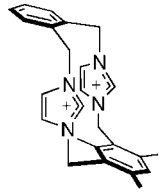

FIGURE 1. The *anti*/*syn* conformation adopted by **4**·2Br in solution and in the solid state.

anti conformers, *and* flip of the benzene rings, which interconverted the *anti* and *syn* conformers. The imidazolium ring rotation process (*anti*→*anti* exchange) was more facile than the benzene ring flip process (*anti*→*syn* exchange), and rate constants and activation energies for each process were estimated from the variable-temperature NMR data (see the first entry in Table 1).[7] The benzimidazolium cyclophane **5**·2Br displayed behavior similar to that of **3**·2Br, including broad signals at room temperature, corresponding to the benzylic protons, that coalesced at higher temperatures.[7,19]

The mesitylene-based cyclophane **4**·2Br displayed very different solution behavior. For solutions of **4**·2Br in DMSO-d_6, sharp signals (including doublets for the benzylic protons) in the ^{1}H NMR spectra at all accessible temperatures indicated the cyclophane to be rigid on the NMR timescale.[7] The cyclophane adopts an *anti*/*syn* conformation, with the imidazolium rings mutually *syn* and the arene rings mutually *anti* (Figure 1). The *anti*/*syn* conformation was also identified in X-ray crystallographic studies.

The azolium cyclophane conformations can be determined by analysis of their ^{1}H NMR spectral data at slow-exchange limits.[1,7,8] The chemical shifts and multiplicities of the signals attributed to the benzylic and imidazolium protons are particularly useful. The magnetic anisotropy of aromatic rings can significantly influence the chemical shifts of nearby protons. For particular conformers, the aromatic groups of the cyclophanes are positioned "above" (or "below") the imidazolium protons and can exert an electronic influence. The expected chemical shift of the imidazolium protons, unaffected by the magnetic anisotropy of nearby aromatic rings, can be based on the chemical shifts of the dibenzylimidazolium cation since the phenyl rings of the benzyl substituents are not positioned such that their magnetic anisotropies should significantly influence the imidazolium protons. The ^{1}H NMR chemical shifts for dibenzylimidazolium chloride, as reported in the literature, are H2 δ 10.79 ($CDCl_3$), 10.04 (DMSO-d_6), 9.49 (D_2O); H4/5 δ 7.34 ($CDCl_3$), 7.97 (DMSO-d_6), 7.70 (D_2O).[20,21] It should be noted that in $CDCl_3$ the signal for the imidazolium H2 proton is considerably downfield (δ 10.79), presumably due to hydrogen bonding to the chloride counteranion. Crabtree and coworkers have reported that the chemical shift of the imidazolium H2 proton in *N*,*N*′-dibutylimidazolium salts can be indicative of ion pairing strength—the stronger the ability of the anion to form hydrogen bonds, the further downfield the H2 signal [δ 10.45 (Br^-), 9.85 (BF_4^-), 8.79 (PF_6^-), and 8.50 (SbF_6^-) in $CDCl_3$].[22]

Results and Discussion

Cyclophane Synthesis. The azolium-linked *ortho* and *ortho*/*meta* imidazolium cyclophanes **8**−**10**, as dibromide salts, were prepared by standard procedures involving the reaction of a bis(imidazolylmethyl)arene with a bis(bromomethyl)arene. The preparations of these salts are reported elsewhere.[7,10,12,15] The butoxybenzimidazolium cyclophane salts **11**·2Br and **12**·2Br were similarly prepared in excellent yield (79−84%) by the reaction of the appropriate 1,2-bis(dibutoxybenzimidazolylmethyl)benzene with 1,2-bis(bromomethyl)benzene. The precursor dibutoxybenzimidazoles, 4,7-dibutoxybenzimidazole and 5,6-dibutoxybenzimidazole, were synthesized in three-step sequences from 1,4-dibutoxybenzene and 1,2-dibutoxybenzene, respectively (Scheme 2). Dinitration of 1,2-dibutoxybenzene afforded 1,2-dibutoxy-4,5-dinitrobenzene,[23,24] which was reduced with hydrazine hydrate and catalytic Pd/C,[25] and the

(20) Harlow, K. J.; Hill, A. F.; Welton, T. *Synthesis* **1996**, 697–698.
(21) Claramunt, R. M.; Elguero, J.; Meco, T. *J. Heterocycl. Chem.* **1983**, *20*, 1245–1249.
(22) Kovacevic, A.; Gründemann, S.; Miecznikowski, J. R.; Clot, E.; Eisenstein, O.; Crabtree, R. H. *Chem. Commun.* **2002**, 2580–2581.
(23) Zhou, Z.-L.; Weber, E.; Keana, J. F. W. *Tetrahedron Lett.* **1995**, *36*, 7583–7586.
(24) Weinberger, L.; Day, A. R. *J. Org. Chem.* **1959**, *24*, 1451–1455.
(25) Rosa, D. T.; Reynolds, R. A., III.; Malinak, S. M.; Coucouvanis, D. *Inorg. Synth.* **2002**, *33*, 112–119.

SCHEME 2. Synthesis of 5,6-Dibutoxybenzimidazole and 4,7-Dibutoxybenzimidazole

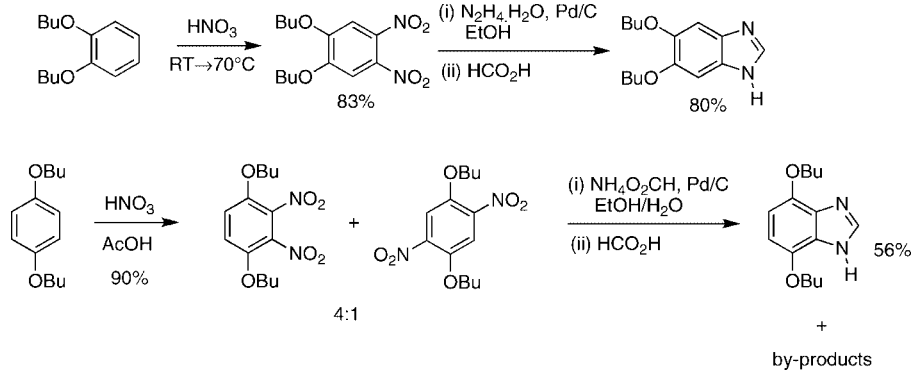

resulting diamine was treated with formic acid[24] to afford 5,6-dibutoxybenzimidazole. 4,7-Dibutoxybenzimidazole was prepared similarly, but dinitration of 1,4-dibutoxybenzene afforded a mixture of isomers, 1,4-dibutoxy-2,3-dinitrobenzene (major) and 1,4-dibutoxy-2,5-dinitrobenzene (minor) in a ratio of ca. 4:1.[26] The mixture was not separated at this step. Reduction of the nitro groups was achieved using ammonium formate and catalytic Pd/C in aqueous ethanol. Careful isolation and purification at the end of the synthetic sequence afforded pure 4,7-dibutoxybenzimidazole.

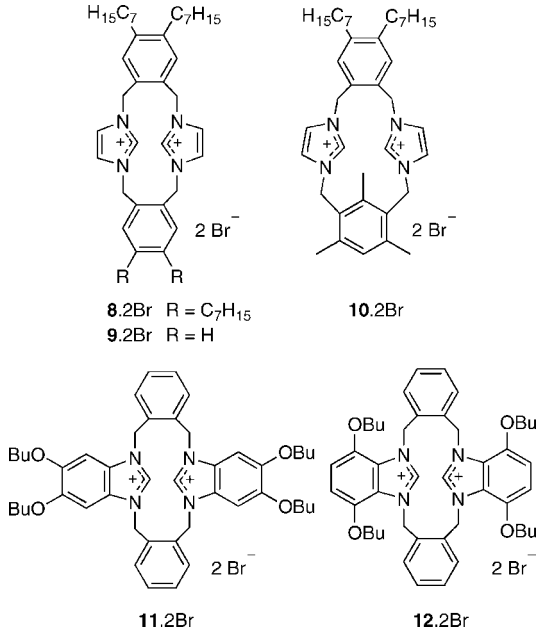

In general, the "non-alkylated" cyclophanes **3**·2Br−**5**·2Br were very soluble in water, displayed low solubility in DMSO and methanol, and were insoluble in organic solvents of medium polarity such as acetone, chloroform, and dichloromethane. The alkylated cyclophanes **8**·2Br−**12**·2Br are much more hydrophobic and exhibit low solubility in water, good solubility in acetone and THF, and excellent solubility in DMSO and methanol. Remarkably, they also exhibit excellent solubility in chloroform and dichloromethane, displaying higher solubility in these solvents than in acetone and THF. In the cases of **8**·2Br−**10**·2Br, the heptyl-substituted cyclophanes, the general trend in solubility is **8**·2Br > **9**·2Br > **10**·2Br. Interestingly, **8**·2BPh$_4$ and **8**·2PF$_6$, which contain counteranions that are typically used to increase solubility of cations in organic media, have solubility in organic solvents lower than that of **8**·2Br. For all the cyclophanes **8**·2Br−**12**·2Br, there is evidence of ion pairing between the (benz)imidazolium H2 protons and the bromide ions in chlorinated solvents (see below). Such ion pairing could make the cyclophanes more soluble in the less polar organic solvents. In the case of the PF_6^- and BPh_4^- salts, ion pairing would be limited, making the salts more ionic in character.

Studies of Conformations in Solutions. Cyclophanes 8·2Br, 8·2PF$_6$, and 9·2Br. The room-temperature ^{1}H NMR spectra of solutions of **8**·2Br and **9**·2Br in DMSO-d_6 or CD_3OD (e.g., Figures 2a and S1−S3 in the Supporting Information) exhibit similar features to ^{1}H NMR spectra for solutions of the non-alkylated analogue **3**·2Br, for example, broad signals corresponding to the benzylic and imidazolium protons. Low-temperature ^{1}H NMR studies of **8**·2Br (in CD_3OD and CH_3OH[27]) indicated that, upon cooling, exchange processes were slowed, and at −70 °C, two different conformers were identifiable from the ^{1}H NMR spectra (Figures 3a and S4−S6 in the Supporting Information), an *anti* conformer (arene rings mutually *anti*), and a *syn* conformer (arene rings mutually *syn*), analogous to the conformers exhibited by **3**·2Br. At −70 °C, both *anti* → *syn* and *anti* → *anti* exchange processes appeared frozen-out. For **8**·2Br in CD_3OD, the ratio of *anti* to *syn* conformers in solution at −70 °C was ca. 0.74:0.26, similar to the ratio of ca. 0.78:0.22 seen for the non-alkylated analogue

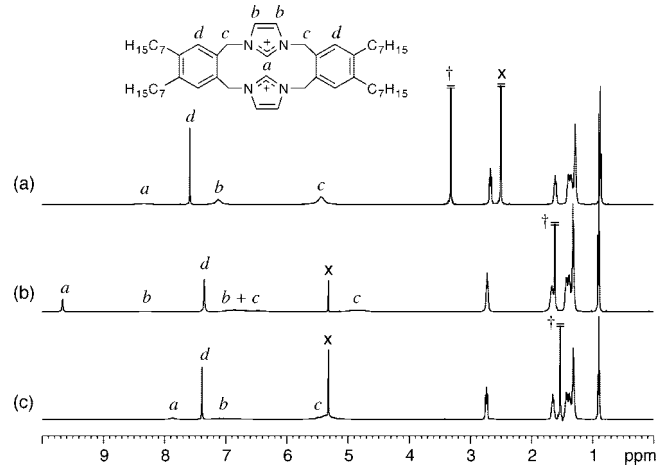

FIGURE 2. ^{1}H NMR spectra (500.1 MHz) of (a) **8**·2Br in DMSO-d_6, (b) **8**·2Br in CD_2Cl_2, and (c) **8**·2PF$_6$ in CD_2Cl_2, all recorded at 25 °C. Key: x = residual solvent signals, † = H_2O.

(26) Kawai, S.; Okawa, Y.; Yada, Y.; Hosoi, H.; Murakoshi, T.; Yajima, I. *Nippon Kagaku Zasshi* **1959**, *80*, 551–555, CAN 55:17958.

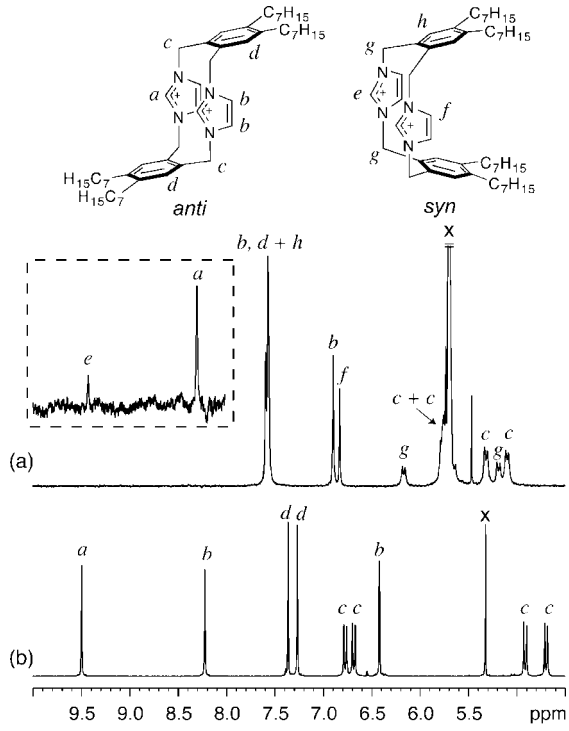

FIGURE 3. Downfield region of the ^{1}H NMR spectra (500.1 MHz) of **8**·2Br (a) in CD_3OD at −70 °C and (b) in CD_2Cl_2 at −40 °C. The region shown in the dashed box is of a spectrum of **8**·2Br in CH_3OH at −70 °C indicating signals for the H2 protons. Key: x = residual solvent signals.

3·2Br in CD_3OD.[7] On warming the solution of **8**·2Br in CD_3OD, the ^{1}H NMR spectra indicated the same behavior that was identified in solutions of **3**·2Br in CD_3OD (see Figures S5 and S6 in the Supporting Information). Initially, a number of the signals attributed to the *anti* conformers began to broaden and eventually coalesced. On further heating, the signals due to the *syn* conformer also broadened and coalesced with the signals from the *anti* conformer. These results are consistent with the operation of two distinct exchange processes, arene ring flip and imidazolium ring rotation, analogous to those in Scheme 1. Rate constants and activation energies for these processes calculated from coalescence temperatures are summarized in Table 1 (see Supporting Information for calculations). The results are comparable to those obtained for the parent cyclophane, **3**·2Br (Table 1).[7]

The above observations suggest that for solutions of **8**·2Br and **9**·2Br in CD_3OD or DMSO-d_6 the alkylated cyclophanes behave similarly to the non-alkylated analogue **3**·2Br, displaying the same exchange processes with similar populations of the different conformers. This result is perhaps not unexpected, given that the alkyl chains are located on the periphery of the cyclophane structure and should not significantly influence the different conformations.

The appearance of the room- and low-temperature ^{1}H NMR spectra for solutions of **8**·2Br (and **9**·2Br) in chloroform and dichloromethane is in stark contrast to their appearance in DMSO and methanol solutions. Detailed NMR studies indicate that the appearance of NMR spectra for solutions containing the cyclophane **8** can be interpreted in terms of the interconversion of the conformers and the ion pairing interactions described in Figure 4. The experiments that lead to these conclusions are summarized below.

Identification of the *anti*/*anti* Conformation of 8 in CD_2Cl_2 Solutions of 8·2Br. Whereas solutions of **8**·2Br and **9**·2Br in DMSO-d_6 display broad signals for the benzylic protons and *all* the imidazolium protons, the room-temperature ^{1}H NMR spectra of **8**·2Br and **9**·2Br in CD_2Cl_2 display very broad signals attributable to the benzylic and imidazolium H4 and H5 protons, but a *sharp*, downfield signal for the imidazolium H2 protons (ca. δ 9.7) (e.g., Figures 2b, and S7 and S8 in the Supporting Information). This result suggests that, for solutions of **8**·2Br in CD_2Cl_2, the processes that interconvert the predominant conformers in solution do not involve a change to the environment of the imidazolium H2 protons.

Low-temperature ^{1}H NMR spectra of **8**·2Br in CD_2Cl_2 indicated the predominance of *only one* conformer at −40 °C (Figures 3b and S9 in the Supporting Information). The signals are sharp, indicating exchange processes to be very slow on the NMR time scale. Two sets of AX patterns for the benzylic protons (i.e., four doublets in total), one singlet for the imidazolium H2 protons, two signals for the imidazolium H4 and H5 protons, and two singlets for the benzene protons suggested one of only two possible conformations (Figure 5), *anti*/*anti* (benzene groups mutually *anti*; imidazolium rings mutually *anti*) or *anti*/*syn* (benzene groups mutually *anti*; imidazolium rings mutually *syn*). Of particular note are the chemical shifts of the imidazolium protons, δ 9.50 (H2) and δ 8.23 and 6.43 (H4 and H5). Compared with the chemical shift of the H2 proton of dibenzylimidazolium chloride (H2 δ 10.79, H4/5 δ 7.34 in $CDCl_3$[20]), the chemical shift of the imidazolium H2 proton of **8**·2Br (δ 9.50 in CD_2Cl_2) is significantly upfield. This upfield shift is consistent with the protons being magnetically shielded by an aromatic ring, a phenomenon that would occur in both the *anti*/*anti* and *anti*/*syn* conformers. Likewise, the chemical shifts of the signals for the imidazolium H4 and H5 protons are significantly different, suggesting that only one of those protons is magnetically shielded by an aromatic ring. The symmetry in cyclophane **8** prevented definitive assignment of which conformer was prevalent at low temperatures, but in the similar cyclophane **9**, the symmetry is reduced.

A low-temperature ^{1}H NMR study of **9**·2Br in CD_2Cl_2 (Figure S10 in the Supporting Information) demonstrated that at −40 °C two similar conformers were present in solution in a ratio of ca. 2.8:1. The ^{1}H NMR data (each conformer exhibited one H2 signal near δ 9.5, four doublets for benzylic protons, and one singlet and an AA′BB′ pattern for the two different benzene rings) are consistent with both conformers being *anti*/*syn* forms (benzene groups mutually *anti*; imidazolium rings mutually *syn*, Figure 6). The identification of which of the two different *anti*/*syn* conformers (A or B in Figure 6) was in highest concentration at −40 °C could not be determined from the ^{1}H NMR spectra for **9**·2Br in CD_2Cl_2.

The structural similarity between **8** and **9** and the similarities in their NMR spectra (cf. Figures S9 and S10 in the Supporting Information) suggest that, in CD_2Cl_2 solution, **8** also exists in the *anti*/*syn* conformation.

Bromide Binding to the *anti*/*anti* Conformation of 8 in CD_2Cl_2 Solutions of 8·2Br. The significance of ion-pairing

(27) The (benz)imidazolium H2 protons undergo rapid H/D exchange with CD_3OD. Throughout our studies, we have also measured ^{1}H NMR spectra of solutions of the cyclophanes in CH_3OH to determine the chemical shift of the H2 protons. However, at room temperature, the H/H exchange of the H2 proton with the hydroxyl proton of CH_3OH is often so rapid that the signal attributed to the H2 proton is too broad to be identified. At low temperatures, the process is slower, and the signal attributed to the H2 protons can be identified.

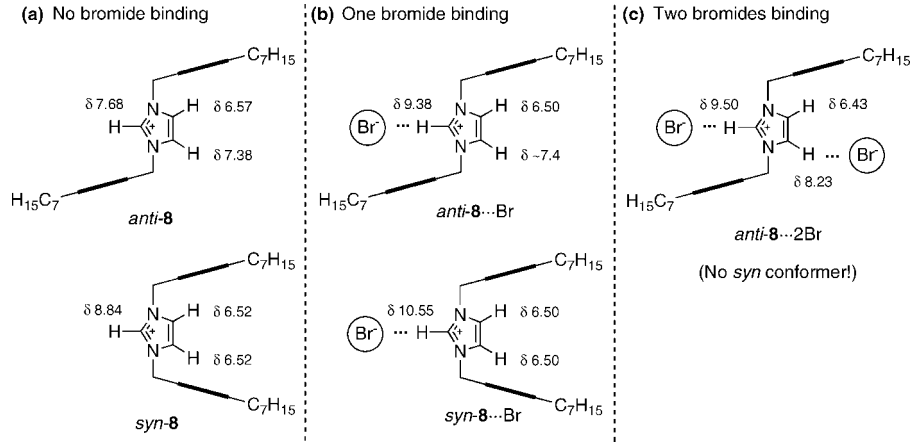

FIGURE 4. Main conformers of **8** and associated bromide binding inferred from ^{1}H NMR spectral data: (a) conformations inferred from spectra of solutions of **8**·2PF$_6$ in CD_2Cl_2 or **8**·2Br in CD_3OD (i.e., in the absence of ion pairing); (b) conformations inferred from spectra of **8**·2PF$_6$ in CD_2Cl_2 with 1 equiv of Bu_4NBr added; and (c) conformations inferred from spectra of CD_2Cl_2 solutions of either **8**·2Br, or **8**·2PF$_6$ with 3 equiv of Bu_4NBr added. Chemical shifts indicated for imidazolium protons were obtained from spectra of (a) a solution of **8**·2PF$_6$ in CD_2Cl_2 at −70 °C, Figure S14 in the Supporting Information; (b) a solution of **8**·2PF$_6$ in CD_2Cl_2 at −40 °C after the addition of 1 equiv of Bu_4NBr, Figure S17 in the Supporting Information; and (c) a solution of **8**·2Br in CD_2Cl_2 at −40 °C, Figure S9 in the Supporting Information.

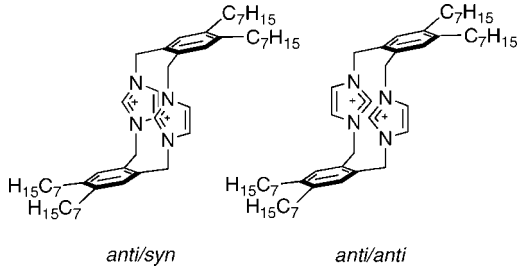

FIGURE 5. Possible low-temperature conformers of **8**·2Br in CD_2Cl_2, based on available ^{1}H NMR data. Comparison with data for **9**·2Br suggested that the predominant conformer for **8**·2Br was the *anti*/*syn* conformer.

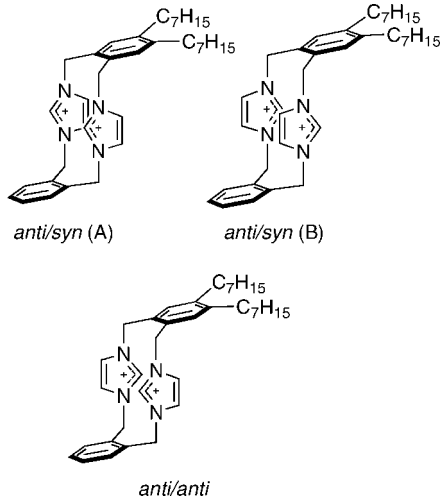

FIGURE 6. Possible low-temperature conformers of **9**·2Br in CD_2Cl_2. ^{1}H NMR data were consistent with the presence of only the *anti*/*syn* conformers.

interactions on the solution behavior of **8** was revealed by a ^{1}H NMR investigation starting with the bromide-free salt **8**·2PF$_6$. The ^{1}H NMR spectra of **8**·2PF$_6$ in methanol and in CD_2Cl_2 were remarkably similar (Figures S11−S14 in the Supporting Information). At low temperatures, both displayed signals consistent with the presence of two different conformers in solution: the *anti* and *syn* conformers identified previously in solutions of **8**·2Br in methanol (*anti*-**8** and *syn*-**8** in Figure 4a). The ratio of the two conformers was ca. 0.81:0.19 (*anti*:*syn*) in methanol and ca. 0.85:0.15 (*anti*:*syn*) in CD_2Cl_2 (cf. 0.75:0.26 *anti*:*syn* for **8**·2Br in methanol).

In the room-temperature ^{1}H NMR spectrum of **8**·2PF$_6$ in CD_2Cl_2 (Figure 2c), the H2 protons appeared as a very broad signal near δ 7.9, but the corresponding signal for the imidazolium H2 protons for **8**·2Br in CD_2Cl_2 as room temperature was sharp and much further downfield (ca. δ 9.5, Figure 2b). The large change in chemical shift for H2 ($\Delta\delta$ = 1.6 ppm) can be attributed to an interaction of a bromide counterion with the imidazolium H2 proton in CD_2Cl_2 solution, which is absent in the more strongly solvating DMSO-d_6 and which has no counterpart in CD_2Cl_2 solutions of **8**·2PF$_6$. A CD_2Cl_2 solution containing **8**·2PF$_6$ and ca. 3 molar equiv of NBu_4Br was analyzed by ^{1}H NMR spectroscopy over a range of temperatures (Figure S15 in the Supporting Information), and the solution behavior of the cyclophane **8** was identical to that of solutions of **8**·2Br in CD_2Cl_2 (Figure S16 in the Supporting Information).

The studies described above suggested that the presence of ion paring between cyclophane **8** and bromide had a significant influence on the solution behavior of **8**. The stoichiometry of binding between the cyclophane and the bromide anions was investigated, initially by the method of continuous variations (Job's method; see Supporting Information).[28] The change in chemical shift for the H2 proton in a sample of **8**·2PF$_6$ in CD_2Cl_2 in response to added bromide was used to generate a Job plot (see Supporting Information). Analysis of this plot suggested that a 1:1 (imidazolium cyclophane **8**/bromide) ion pair existed in solution.

To further explore this 1:1 ion pairing, a solution of **8**·2PF$_6$ with 1 equiv of NBu_4Br in CD_2Cl_2 was examined by variable-temperature ^{1}H NMR spectroscopy. The ^{1}H NMR spectrum recorded at −40 °C (Figure S17a in the Supporting Information) displayed signals consistent with two species—one *anti* conformer and one *syn* conformer (ca. 0.8:0.2 *anti*:*syn*)—the dynamic process that interconverts the species being frozen out

(28) (a) Connors, K. A. *Binding Constants. The Measurement of Molecular Complex Stability*; John Wiley & Sons: New York, 1987. (b) Schneider, H.-J.; Yatsimirsky, A. *Principles and Methods in Supramolecular Chemistry*; John Wiley & Sons: Chichester, UK, 2000.

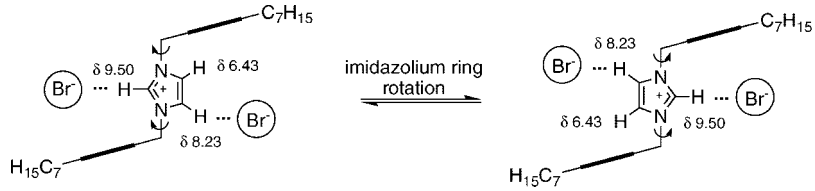

FIGURE 7. Predominant conformers in CD_2Cl_2 solution of **8**·2Br and the imidazolium ring rotation process that converts the two conformers.

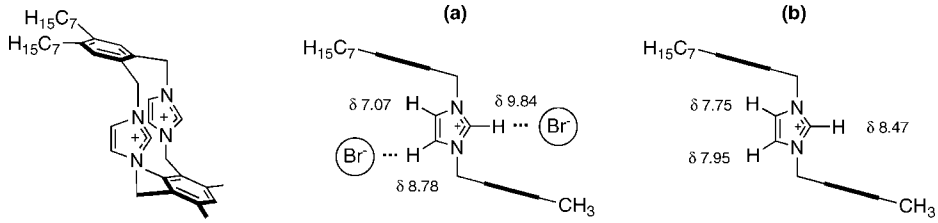

FIGURE 8. Selected ^{1}H NMR chemical shift data for **10**·2Br in (a) $CDCl_3$ and (b) DMSO.

at this temperature. The NMR signals for both conformers were consistent with only the H2 protons being involved in interactions with bromide ions (e.g., *anti*-**8**···Br and *syn*-**8**···Br in Figure 4b). The only significant differences between the chemical shift data for *anti*-**8** and *anti*-**8**···Br, or *syn*-**8** and *syn*-**8**···Br, is the downfield shift of the signal for the imidazolium H2 protons ($\Delta\delta$ = 1.7 ppm in each case, cf. Figure 4a,b). However, despite the Job plot indicating a 1:1 binding stoichiometry between **8** and bromide, the ^{1}H NMR spectra of a solution of **8**·2PF_6 with 1 equiv of NBu_4Br in CD_2Cl_2, that is, consisting of *anti*-**8**···Br and *syn*-**8**···Br, were not the same as the ^{1}H NMR spectra of solutions of **8**·2Br in CD_2Cl_2.

The only significant difference in ^{1}H NMR chemical shifts of *anti*-**8**···Br in Figure 4b (from a solution of **8**·2PF_6 in CD_2Cl_2 after the addition of 1 equiv of NBu_4Br) and *anti*-**8** in Figure 4c (the only conformer detected in solutions of **8**·2Br in CD_2Cl_2 at −40 °C) is the downfield shift of the signal for one of the imidazolium H4/5 protons (δ ~7.4 → δ 8.23; $\Delta\delta$ = 0.83 ppm). This difference is consistent with the imidazolium H4/5 protons interacting with an additional bromide ion when more than 1 equiv of bromide is present. In solutions of **8** in CD_2Cl_2 in the presence of 2 or more equiv of bromide, the only cyclophane species observed in solution is an *anti* conformer ion pairing with *two* bromide ions, denoted as *anti*-**8**···2Br (Figure 4c). Presumably, unfavorable steric interactions that would accompany the binding of the second bromide ion to protons on the "back" of the imidazolium ring prevents the observation of a *syn* conformer (i.e., *syn*-**8**···2Br).

In summary, there are two binding events for the cyclophane **8**. In the first binding event, bromide binds to H2, while in the second binding event, which only occurs after H2 is saturated, bromide binds to H4/5. The analysis by Job's method probes the first binding event at room temperature. The second binding event involves changes in signals that are too broad at room temperature to be analyzed. As a result, the Job's method indicated a 1:1 binding stoichiometry (first binding event) while the subsequent low-temperature investigation indicated an overall 1:2 stoichiometry (first and second binding events).

It is interesting to consider the consequences of the ion pairing. When ion pairing involves two bromide anions (as for **8**·2Br in CD_2Cl_2), only one conformer of **8** is detectable in solution, the interaction of the bromide anions favoring the *anti* conformer *anti*-**8**···2Br, whereas both *anti* and *syn* conformations are seen when ion pairing involves only one bromide. The kinetics for the conformational exchange processes are also significantly influenced by bromide binding. Analysis of the variable-temperature ^{1}H NMR spectra for **8**·2Br in CD_2Cl_2 (Figures S16 in the Supporting Information) permitted only determination of the imidazolium ring rotation process (interconversion of the two *anti* conformers, Figure 7). From coalescence information, we estimate the rate constant for the *anti* → *anti* exchange process to be 104 ± 4 s^{-1} at 5 °C and the free energy of activation for this process to be 57 ± 1 kJ mol^{-1} (see Supporting Information for calculations). A comparison of the kinetic data is presented in Table 1. When the cyclophane **8** is ion-paired with two bromide anions, as for *anti*-**8**···2Br (entry 3, Table 1), the rate constant for the imidazolium ring rotation process is much lower and the free energy of activation for this process is much higher—by ca. 10 kJ mol^{-1}—than in the absence of any cyclophane−bromide pairing (entries 1, 2, and 4 in Table 1). It could be envisaged that, with bromide binding to the imidazolium protons, the bromide ions "hold" the imidazolium rings in the *anti* conformation, a higher energy being required to break the imidazolium···bromide interaction before imidazolium ring rotation can occur (Figure 7). Similarly, bromide binding slows the arene "ring flip" process that interconverts *anti* and *syn* conformations of **8**. Thus, whereas coalescence of benzylic signals for **8** in the absence of bromide (Figures S19−S22 in the Supporting Information) is indicative of interconversion of *anti* and *syn* conformations, in the presence of bromide (Figure S16 in the Supporting Information), while benzylic signals of **8** showed some broadening at high temperature, coalescence did not occur at accessible temperatures. Alcalde et al. have observed a similar "braking" effect for an imidazolium-linked *meta*-xylyl cyclophane where the signals for the benzylic protons of the cyclophane appeared as a singlet in the presence of chloride or trifluoroacetate but appeared as two pairs of doublets in the presence of hydroxide.[6]

Cyclophane 10·2Br. The solution behavior of **10**·2Br in DMSO-d_6 at room temperature was similar to that of the nonalkylated analogue **2**·2Br. The ^{1}H NMR spectra suggest that, not unexpectedly, the only conformation seen for **10**·2Br in DMSO-d_6 solution was the *anti*/*syn* arrangement (Figure 8). The ^{1}H NMR spectra (Figure S23 in the Supporting Information) displayed sharp signals, including four doublets for the benzylic protons and a sharp singlet for the imidazolium H2 protons (at δ 8.47), consistent with *anti*/*syn* conformer being rigid on the NMR time scale. The upfield chemical shift of the imidazolium H2 proton signal (δ 8.47, cf. δ 10.04 for dibenzylimidazolium

chloride in DMSO-d_6) suggests that the imidazolium H2 protons are affected by magnetic shielding from a nearby aromatic ring. The spectra of **10**·2Br in methanol exhibit some interesting differences compared to the spectra of DMSO-d_6 solutions. The set of doublets corresponding to the benzylic protons of the *ortho*-xylyl group is slightly broadened at room temperature (see Figures S24 and S25 in the Supporting Information), while the doublets for the benzylic protons on the mesitylene group are sharp. The signal attributed to the imidazolium H2 proton (seen in CH_3OH solutions, but not seen in CD_3OD solutions) is broad at room temperature, but sharp at lower temperatures (Figures S26 in the Supporting Information). A number of signals broaden slightly as the temperature is lowered to 10 °C and then sharpen as the temperature is lowered further, beyond −10 °C, but these effects are not accompanied by substantial changes in chemical shifts or changes in the number of signals detected. We do not know the cause of these subtle changes in the variable-temperature NMR spectra of **10**·2Br in methanol.

The spectra of **10**·2Br in $CDCl_3$ (see Figure S27 in the Supporting Information) exhibit some differences compared to the spectra of the DMSO-d_6 or methanol solutions. The spectra exhibit sharp signals independent of temperature, indicating a structure that is rigid on the NMR time scale. Saturation transfer ^{1}H NMR experiments on **10**·2Br in $CDCl_3$ at 40 °C showed no evidence of slow exchange processes. The chemical shifts of the signals for the imidazolium H4 and H5 protons are significantly different in the two solvents ($\Delta\delta$ 1.71 ppm in $CDCl_3$, cf. $\Delta\delta$ 0.2 ppm in DMSO-d_6), and those of the imidazolium H2 protons are significantly further downfield in $CDCl_3$ (δ 9.84, cf. δ 8.47 in DMSO-d_6). These data are consistent with an *anti*/*syn* conformation for **10** in both $CDCl_3$ and DMSO-d_6, but in $CDCl_3$ with the presence of hydrogen bonding between the imidazolium protons and bromide ions (Figure 8), as was observed for **8**.

Cyclophanes 11·2Br and 12·2Br. The butoxy-substituted benzimidazolium cyclophanes **11** and **12** display significantly different solution behavior compared to their imidazolium analogues **8** and **9** discussed previously. In addition, the structural variations between **11** and **12** result in these cations exhibiting significantly different solution behaviors to each other and, in the case of **12**, induce a conformation not previously identified for imidazolium/benzimidazolium cyclophanes linked by *ortho*-xylyl groups.

At room temperature, solutions of **11**·2Br in DMSO-d_6 and methanol (Figures S28 and S29 in the Supporting Information) exhibited numerous broad signals over the entire ^{1}H NMR spectrum. The signals were consistent with multiple conformers undergoing exchange processes. Only in the case of the DMSO solution could the temperature be raised sufficiently to achieve coalescence of signals. The high freezing point of DMSO meant that the slow exchange limit for spectra of **11** could not be reached, so that the nature and relative populations of each of the conformers could not be determined. ^{1}H NMR spectra of methanol solutions containing **11**·2Br at −10 °C were sharp (Figures S29 and S30 in the Supporting Information) and consistent with the presence of two conformers in solution—a *syn* and an *anti* conformer (Figure 9) in the ratio of ca. 0.75:0.25, respectively. The conformers were identified by the numbers, patterns, and chemical shifts of the signals in the ^{1}H NMR spectra. Of particular note are the chemical shifts (Figure 9) of the benzimidazolium H2 protons (δ 7.41 for the *syn* conformer and δ 8.61 for the *anti*) and the protons on the fused benzo ring of the benzimidazolium moiety (δ 7.25 for the *syn* conformer and δ 6.13 and 7.32 for the *anti*).

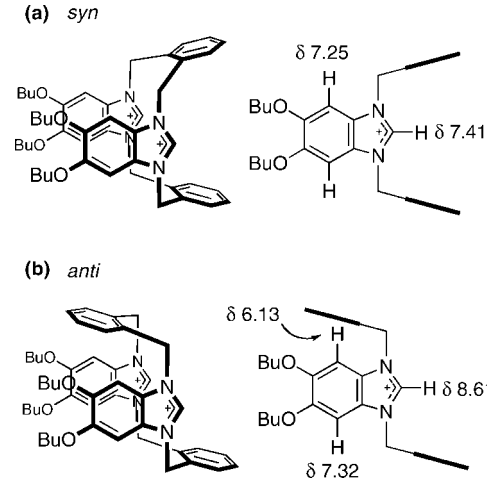

FIGURE 9. Two conformers of **11** and selected chemical shifts from solutions of **11**·2Br in methanol at −10 °C.

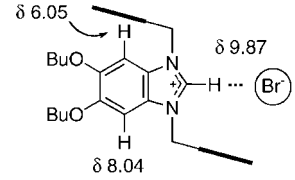

FIGURE 10. Only conformation of **11** (with pertinent ^{1}H chemical shifts) detected in solutions of **11**·2Br in CD_2Cl_2 at room temperature.

The room-temperature ^{1}H NMR spectra for solutions of **11**·2Br in CD_2Cl_2 (Figure S31 in the Supporting Information) exhibited sharp signals consistent with only one major conformer in solution (the *anti* conformer in Figure 10). The downfield chemical shift of the benzimidazolium H2 proton (δ 9.87, Figure 10) is consistent with the presence of hydrogen bonding between the proton and a bromide anion. The signal is significantly downfield ($\Delta\delta$ 1.3) by comparison with the chemical shift for the equivalent proton of the *anti* conformer in methanolic solutions (δ 8.61, Figure 9). It is interesting to note that in methanol the predominant conformer is the *syn* conformer, yet in the presence of bromide binding (in chlorinated solvents), the *anti* conformer is predominant. It may be that the steric bulk of the bromide ion destabilizes the *syn* conformation, where binding of bromide to H2 would wedge the bromide ion between two aromatic rings.

Saturation-transfer ^{1}H NMR experiments were conducted to explore the possibility of slow-exchange processes involving the *anti* conformer in solutions of **11**·2Br in CD_2Cl_2 at 30 °C (Figure S32 in the Supporting Information). Saturation of one of the signals due to aromatic protons on the fused benzo ring of the benzimidazolium moiety (e.g., δ 6.0, Figure 11) resulted in a significant decrease in the intensity of the signal attributed to the other proton on the benzo ring of the benzimidazolium moiety (e.g., δ 8.0, Figures 11 and S32 in the Supporting Information). Saturation of the signals corresponding to the *exo* (or *endo*) benzylic protons did not change the intensity of the signals for the corresponding *endo* (or *exo*) benzylic protons by any appreciable amount. These results suggests that (i) the benzimidazolium rings are undergoing partial rotation about their N−N axes, interconverting two *anti* conformers in a process that exchanges the environments of the two aromatic protons

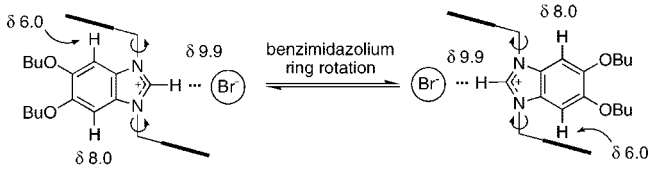

FIGURE 11. Benzimidazolium ring rotation (about the N−N axis) that interconverts the two *anti* conformers of **11**, as suggested by ^{1}H NMR saturation transfer studies of solutions of **11**·2Br at room temperature.

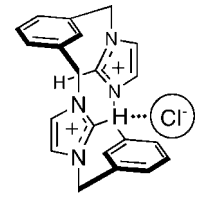

13···Cl

FIGURE 13. The *anti*/*anti* conformer adopted in the solid state by **13**.[2]

on the benzo-fused ring (Figure 11), but (ii) arene ring flip processes that would exchange the environments of the benzylic protons are not occurring at a measurable rate.

The room-temperature ^{1}H NMR spectra of solutions of **12**·2Br in DMSO-d_6 (Figure 12) exhibit sharp signals for the phenyl protons (of the xylyl and benzimidazolium groups) and the benzimidazolium H2 protons, but broadened doublets for the benzylic protons, as well as broadened signals corresponding to the methylene protons of the butyl chains. Of particular note is the upfield chemical shift of the H2 proton (δ 7.11, Figure 12), which is consistent with magnetic shielding of this proton by two aromatic rings. The spectra are consistent with **12** existing in a *syn* conformation. On heating the DMSO-d_6 solutions, coalescence of the benzylic signals occurs (at ca. 70 °C), the signals for the methylene protons of the butyl chain becomes sharp, and *all* other signals remain the same (Figure 12). These results are consistent with the existence of an exchange process that interconverts two equivalent *syn* conformations of **12** (Figure 12). This exchange process results in the environments of the benzylic protons to be interchanged and the environments of the diastereotopic methylene protons of the butyl chains also being interchanged, while the environments of other protons are unaffected. This exchange presumably occurs via a combination of both benzimidazolium ring rotation and benzene ring flip processes, with other conformers as (undetected) intermediates. The effective rate constant for the interconversion of the two *syn* conformers is estimated at 719 ± 9 s^{-1} at 70 °C with an activation energy of 66 ± 2 kJ mol^{-1}.

Interestingly, the ^{1}H NMR spectra of **12**·2Br in methanol display sharp signals over a broad temperature range consistent with a single frozen-out conformation (*syn*). (The spectrum shown in Figure S34 in the Supporting Information is representative of the spectra over the broad temperature range.) At 50 °C, the benzylic doublets start to broaden, suggesting the occurrence of very slow exchange processes. The signal for the benzimidazolium H2 proton (δ 7.2), observable in CH_3OH solutions, is sharp only at low temperature being broadened at high temperatures, presumably due to rapid H−H exchange with the methanol hydroxyl proton. The spectral features are suggestive again of only a single *syn* conformer in solution. The ^{1}H NMR spectra of **12**·2Br in $CDCl_3$ (Figure S35 in the

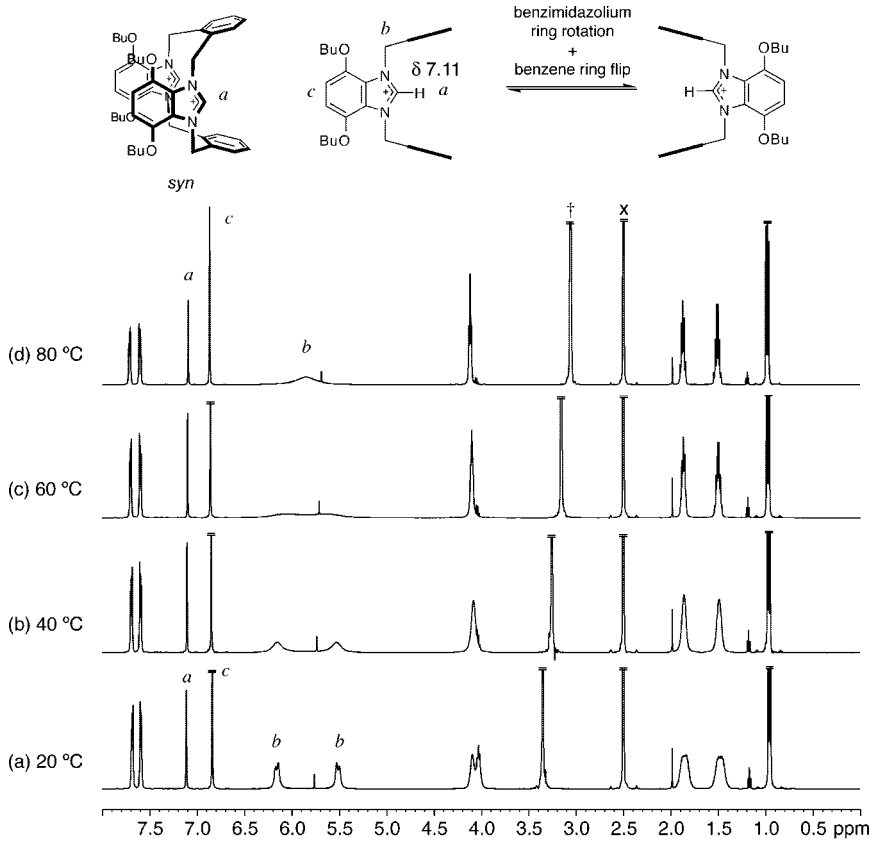

FIGURE 12. Variable-temperature ^{1}H NMR spectra (500.1 MHz, DMSO-d_6) of **12**·2Br. Key: x = residual solvent signal, † = H_2O. See Figure S33 in the Supporting Information for additional spectra.

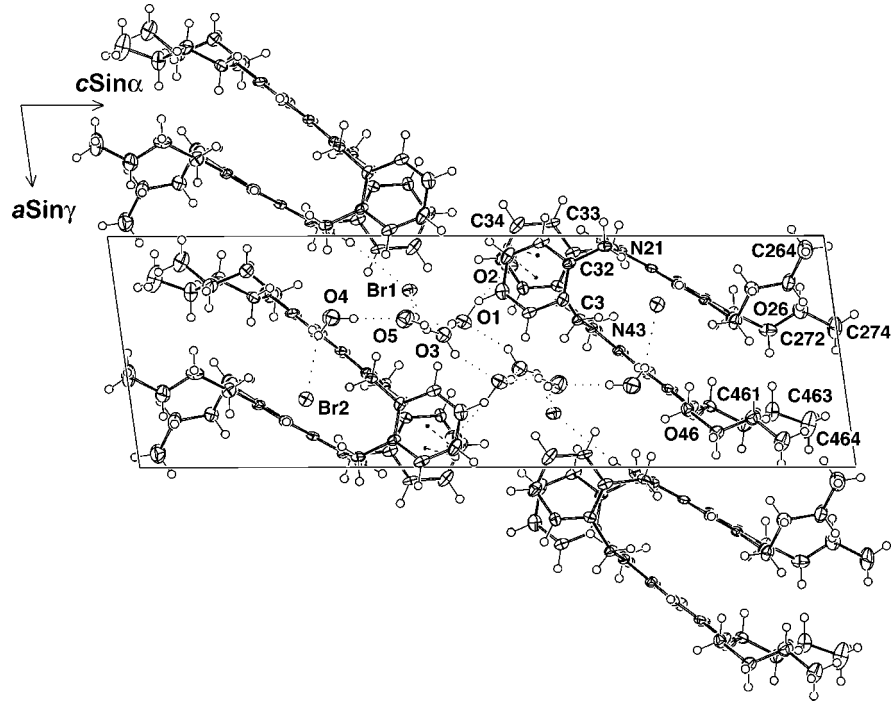

FIGURE 14. Unit cell contents of **11**·2Br·5H_2O, projected down *b*, showing hydrogen bonding.

Supporting Information) are almost identical to those in methanol. The signal for the benzimidazolium H2 proton of **12** is still relatively upfield (δ 7.2), consistent with the H2 protons being magnetically shielded by two benzene rings (i.e., a *syn* conformation for **12**) and not being involved in ion pairing interactions with bromide counterions. Presumably, the butyl substituents in **12** favor the *syn* conformation of the cyclophane by sterically hindering the approach of the benzene groups to the benzimidazolium groups. In the *syn* conformation, the benzene groups prevent approach of bromide ions to the H2 protons, thereby eliminating ion-pairing effects at the H2 site. Saturation transfer experiments conducted for a solution of **12**·2Br in $CDCl_3$ suggest the existence of an exchange process that interconverts two equivalent *syn* conformations (Figure 12), but which was only detectable at temperatures above room temperature.

The benzimidazolium cyclophanes **11** and **12** are the only *ortho*-xylyl-linked imidazolium/benzimidazolium cyclophanes that have exhibited *syn* conformers where the azolium C2−H2 bond points into the cavity between aromatic rings. These two cyclophanes also adopt the *syn* conformation in preference to an *anti* conformation, whereas for other *ortho*-xylyl-linked imidazolium cyclophanes, the *anti* conformation is dominant. The benzimidazolium cyclophanes **11** and **12** also display some of the slowest dynamic behavior identified for *ortho*-xylyl-linked imidazolium/benzimidazolium cyclophanes.

Solid-State Structural Studies. Attempts to grow crystals of **8**·2Br or **8**·2PF_6 suitable for crystallographic studies proved unsuccessful. It was, however, possible to grow crystals of the tetraphenylborate salt **8**·2BPh_4, although the limited solubility of the salt prevented low-temperature ^{1}H NMR studies of solutions of the salt. It is interesting to note that, despite the dominant solution conformer of **8** (regardless of counteranion or solvent) being *anti*/*syn* (arenes mutually *anti* and imidazolium rings mutually *syn*), in the solid-state crystallographic study of **8**·2BPh_4, the cyclophane adopts an *anti*/*anti* conformation (Figure S51 in the Supporting Information). One half of the formula unit comprises the asymmetric unit in a triclinic $P\bar{1}$ unit cell, and an inversion center lies between the pair of imidazolium rings. Alcalde et al. have reported the solid-state structure of an imidazolium-linked *meta*-xylyl cyclophane (**13**), which, when crystallized as the chloride salt, adopted a *anti*/*anti* conformation with one imidazolium H2···chloride hydrogen bond (as displayed in Figure 13).[2]

The present studies of the bromide salts of **11** and **12** are modeled in terms of adducts which are quite heavily hydrated, **11**·2Br·5H_2O and **12**·2Br·4H_2O, all hydroxylic hydrogen atoms being located in difference maps (**11**·2Br·5H_2O) or refinable in $(x,y,z,U_{iso})_H$ (**12**·2Br·4H_2O). In **11**·2Br·5H_2O (where one formula unit, devoid of crystallographic symmetric, comprises the asymmetric unit of the structure), the two imidazole hydrogen atoms contact a bromide ion (H···Br 2.92 Å (est.)) and a water molecule oxygen atom (H···O 2.32 Å (est.)), a hydrogen-bonded column being formed parallel to *b* (Figure 14). Interestingly, water molecule 2 is "sandwiched" between the phenyl rings (H···centroid distances 2.4_3, 2.6_8 Å (est.)) with the centroid−centroid distance being 6.0_5 Å (est.) (Figure 15). In **12**·2Br·4H_2O, where only one imidazole hydrogen atom is crystallographically independent (the cation being disposed about a crystallographic 2-axis in monoclinic space group *C*2/*c*), the contact is to a bromide ion (H···Br 3.08(3) Å). Here, no entity is sandwiched, the intercentroid distance being 4.9_4 Å and the phenyl rings obligate parallel (Figure S53 in the Supporting Information). The cations pack in columns parallel to *c*, with a pronounced layering normal to that axis, consisting of alternate sheets of cations interspaced by anions and solvent molecules, hydrogen-bonded (Figure S49 and S50 in the Supporting Information). Full details of hydrogen bonding schemes for **11**·2Br·5H_2O and **12**·2Br·4H_2O are given in the Supporting Information. The crystal packing in **8**·2BPh_4 is also of interest in that the heptyl substituents are disposed parallel to and either side of the *ab* plane, the latter layering the structure (Figure S54 in the Supporting Information). The anions embrace pairwise about inversion centers (1/2, 0, 1/2).

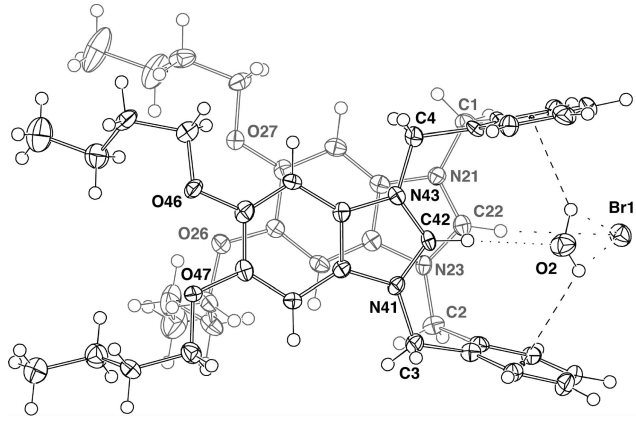

FIGURE 15. Projection of the cation **11**, with associated anion and water molecules (see also Figure S52 in the Supporting Information).

The phenyl rings of the cation are surrounded by those of the anion in edge-to-face contact.

Conclusions

The structure of azolium-linked cyclophanes, the types of counteranions, and the particular solvents in which the cyclophanes are studied can have a significant influence on the conformers observed and the rates of the processes that may interconvert them. The incorporation of alkyl chains onto the periphery of the imidazolium cyclophanes has extended the solubility of the cyclophanes to allow studies in chlorinated solvents. With noncoordinating counteranions, the solution behaviors of the alkylated cyclophanes in chlorinated solvents were found to be similar to that of the cyclophanes with bromide counteranions in polar solvents such as methanol and DMSO. In chlorinated solvents, however, the presence of bromide counteranions impacts on the behavior of the cyclophanes. Thus, in the case of the *ortho*-linked imidazolium cyclophane **8**, only a single *anti* conformer was detected in solution, with the cyclophane forming ion pairs with two bromide anions. Not only did the bromide ions influence the solution conformation but the cyclophane···bromide interactions significantly impacted the activation barrier for the processes that interconvert the solution conformers, by making rotation of the imidazolium rings about their N−N axes more difficult.

In the case of the butoxy−benzimidazolium systems, the position of the butoxy fictionalization has a significant influence on the conformations adopted by the cyclophanes. Particularly in the case of **12**, the preferred conformer is a *syn* conformer where the benzimidazolium H2 protons are directed into the cavity formed by the two *ortho*-xylyl groups. This is the first time such a conformation has been identified for azolium-linked *ortho*-cyclophanes and suggests interesting possibilities with respect to the formation of N-heterocyclic carbene metal complexes derived from such carbene precursors. We are currently exploring the metal complexation of N-heterocyclic carbenes derived from these benzimidazolium cyclophanes and related species.

Experimental Section

General Procedures and Materials. General experimental procedures have been described previously.[12,16] The synthesis of the cyclophane salts **8**·2Br, **9**·2Br, and **10**·2Br has been reported previously, though an improved synthesis of **8**·2Br is reported here.[7,10,12,15] 1,2-Bis(bromomethyl)-1,2-diheptylbenzene and 1,2-bis(imidazol-1-ylmethyl)-4,5-diheptylbenzene were prepared by the method of Baker et al.[12] 1,2-Dibutoxy-4,5-dinitrobenzene[23,24] and crude 1,4-dibutoxy-2,3-dinitrobenzene[26] (as a mixture containing ca. 20 mol % of 1,4-dibutoxy-2,5-dinitrobenzene) were prepared by literature procedures. Where detailed assignment of ^{13}C NMR spectra is provided below, these assignments have been made with the aid of HSQC (1-bond $^{1}H-^{13}C$ correlation) and HMBC (2/3-bond $^{1}H-^{13}C$ correlation) 2D NMR experiments.

Full ^{1}H NMR details for the imidazolium and benzimidazolium cyclophanes are provided in Supporting Information.

1,1′,3,3′-Bis(4,5-diheptyl-*o*-xylyl)diimidazolium dibromide 8·2Br. Solutions of 1,2-bis(imidazol-1-ylmethyl)-4,5-diheptylbenzene (1.0 g, 2.3 mmol) in acetone (50 mL) and crude 1,2-bis(bromomethyl)-1,2-diheptylbenzene (1.06 g) in acetone (50 mL) were added portionwise, simultaneously, to acetone (180 mL) heated at reflux over the course of 5 h. The mixture was then heated at reflux for 4 days. The volume of solvent was concentrated by ca. 120 mL and then cooled to rt. The resulting precipitate was collected, washed with acetone, and dried to afford a white powder (1.09 g, 53%): $C_{50}H_{78}N_4Br_2 \cdot 2H_2O$ requires C, 64.50; H, 8.88; N, 6.02%. Found: C, 64.71; H, 9.04; N, 5.95; δ_C ($CDCl_3$, 125.8 MHz, 298 K) 14.0 (CH_3), 22.6, 29.0, 29.7, 30.8, 31.7, 32.3 (6 × CH_2), 51.7 (br, benzylic CH_2), 119.9 (v br), 124.3 (v br), 128.6 (v br), 134.6 (CH), 135.6 (CH), 145.0 (v br); *m*/*z* (ES CH_2Cl_2) 813.5225 (M − Br) ($C_{50}H_{78}N_4{}^{81}Br$ requires 813.5233).

1,1′,3,3′-Bis(4,5-diheptyl-*o*-xylyl)diimidazolium bis(hexafluorophosphate) 8·2PF$_6$. A solution of **8**·2Br (257 mg, 0.29 mmol) in methanol (25 mL) and water (10 mL) was added to a solution of potassium hexafluorophosphate (0.7 g, 3.8 mmol) in methanol (25 mL) and water (10 mL). The mixture was stirred for 1 h and was then diluted with water (40 mL). The resulting precipitate was collected, washed with water (20 mL), and dried to afford a white powder (255 mg, 86%). $C_{50}H_{78}N_4P_2F_{12} \cdot 0.1H_2O$ requires C, 58.48; H, 7.68; N, 5.46%. Found: C, 58.09; H, 7.95; N, 5.14.

We have previously reported the synthesis of **8**·2Br and **8**·2BPh$_4$ and the mass and NMR [in $(CD_3)_2SO$ solutions] spectral data of **8**·2Br.[10] Single crystals of **8**·2BPh$_4$ suitable for X-ray diffraction studies were grown by slow evaporation of an acetone solution of the cyclophane.

5,6-Dibutoxybenzimidazole (14). Hydrazine hydrate (41 mL, 0.84 mol) was added slowly to a stirred mixture of 1,2-dibutoxy-4,5-dinitrobenzene (26.5 g, 85 mmol) and palladium on carbon (0.59 g, 10% Pd/C) in ethanol (250 mL). After the addition was complete, the mixture was heated at reflux for 14 h. The mixture was cooled and filtered through Celite under a nitrogen atmosphere. The filtrate was concentrated in vacuo to afford a yellow solid (ca. 21 g of crude 1,2-dibutoxy-4,5-diaminobenzene). The solid was dissolved in formic acid (100 mL, 90%), and the resulting solution was heated at reflux for 3 h. The mixture was diluted with aqueous ammonia solution (50 mL, 28%) and then aqueous sodium carbonate solution (140 g in 1000 mL). The resulting precipitate was collected, washed with water (2 × 100 mL), and air-dried to afford a pale brown solid. The solid was dissolved in toluene (250 mL), and the mixture was dried by azeotropic distillation of water. The resulting toluene solution was concentrated to ca. 150 mL and diluted with hexanes (50 mL). The resulting precipitate was collected, washed with hexanes (100 mL), and dried to afford a pale brown powder (18 g, 80%). $C_{15}H_{22}N_2O_2$ requires C, 68.67; H, 8.45; N, 10.68%. Found: C, 68.73; H, 8.50; N, 10.49; δ_H [$(CD_3)_2SO$, 300.1 MHz] 0.94 (6H, t, $^{3}J_{H,H}$ 7.4 Hz, 2 × CH_3), 1.47 (4H, m, 2 × CH_2CH$_3$), 1.71 (4H, m, 2 × OCH$_2$CH_2), 3.95 (4H, t, $^{3}J_{H,H}$ 6.4 Hz, 2 × OCH_2), 7.03 and 7.16 (2H, 2 × br s, 2 × Ar H), 7.98 (1H, s, NCHN), and 12.1 (1H, s, NH); δ_C [$(CD_3)_2SO$, 75.5 MHz] 13.8 (CH_3), 18.8 (CH_2), 31.0 (CH_2), 68.7 (OCH_2), 96.6 (br, Ar C), 104.1 (br, Ar C), 127.1 (br, Ar C), 136.7 (br, Ar C), 140.3 (NCHN), 145.6 (br, Ar C), and 146.5 (br, Ar C).

1,2-Bis(5′,6′-dibutoxybenzimidazolyl-1′-methyl)benzene (15). Sodium hydride (0.6 g, 15 mmol; 60% dispersion in oil) was added

to a solution of 5,6-dibutoxybenzimidazole (**14**) (3.36 g, 12.8 mmol) in dry THF (150 mL). The mixture was stirred for 30 min. To the resulting solution was added a solution of 1,2-bis(bromomethyl)-benzene (1.69 g, 6.4 mmol) in dry THF (30 mL). The mixture was then heated at reflux for 18 h. The mixture was cooled and then filtered through a plug of Celite and basic alumina. The filtrate was concentrated in vacuo, and the residue was triturated with hot hexanes (150 mL) to afford a white solid (3.65 g, 91%). $C_{38}H_{50}N_4O_4$ requires C, 72.81; H, 8.04; N, 8.94%. Found: C, 72.72; H, 8.12; N, 8.70; δ_H ($CDCl_3$, 300.1 MHz) 0.94 (6H, t, $^3J_{H,H}$ 7.4 Hz, 2 × CH_3), 0.97 (6H, t, $^3J_{H,H}$ 7.4 Hz, 2 × CH_3), 1.49 (8H, m, 4 × CH_2CH_3), 1.74 (4H, m, 2 × OCH_2CH_2), 1.81 (4H, m, 2 × OCH_2CH_2), 3.80 (4H, t, $^3J_{H,H}$ 6.5 Hz, 2 × OCH_2), 4.01 (4H, t, $^3J_{H,H}$ 6.5 Hz, 2 × OCH_2), 5.17 (4H, s, 2 × benzylic CH_2), 6.48 (2H, s, 2 × benzimidazole Ar CH), 7.03−7.10 (2H, AA′ part of AA′XX′ pattern, xylyl Ar 3-CH and 6-CH), 7.27 (2H, s, 2 × benzimidazole Ar CH), 7.30−7.37 (2H, XX′ part of AA′XX′ pattern, xylyl Ar 4-CH and 5-CH), and 7.64 (2H, s, 2 × NCHN); δ_C ($CDCl_3$, 75.5 MHz) 13.8 (CH_3), 19.18 (CH_2CH_3), 19.23 (CH_2CH_3), 31.22 (CH_2), 31.24 (CH_2), 46.4 (benzylic CH_2), 69.3 (OCH_2), 69.5 (OCH_2), 94.7 (benzimidazole CH), 104.3 (benzimidazole CH), 127.6 (benzimidazole C), 129.16 (xylyl Ar CH C3/6), 129.22 (xylyl Ar CH C4/5), 133.1 (xylyl Ar C C1/2), 137.1 (benzimidazole C), 141.0 (NCHN), 147.1 (benzimidazole C−O), and 147.8 (benzimidazole C−O).

1,1′,3,3′-Bis(*o*-xylyl)bis(5′,6′-dibutoxybenzimidazolium) dibromide 11·2Br. Solutions of 1,2-bis(5′,6′-dibutoxybenzimidazolylmethyl)benzene (**15**) (1.67 g, 2.7 mmol) in acetone (50 mL) and 1,2-bis(bromomethyl)benzene (0.716 g, 2.7 mmol) in acetone (50 mL) were added portionwise, simultaneously, to acetone (200 mL) heated at reflux over the course of 7 h. The mixture was then heated at reflux overnight. The volume of solvent was concentrated by ca. 100 mL and then cooled to rt. The resulting precipitate was collected, washed with acetone, and dried to afford a white powder (1.9 g, 79%), which can be recrystallized from methanol/water solutions. $C_{46}H_{58}N_4O_4Br_2\cdot 2H_2O$ requires C, 59.61; H, 6.74; N, 6.05% Found: C, 59.43; H, 6.51; N, 5.77; δ_C ($CDCl_3$, 75.5 MHz) 13.8 and 14.0 (CH_3), 19.1 and 19.3 (CH_2CH_3), 30.8 and 31.0 (CH_2), 50.7 and 52.0 (benzylic CH_2), 69.6 and 70.4 (OCH_2), 96.3 and 97.4 (benzimidazolium CH), 123.8 and 125.9 (benzimidazolium C), 132.3 and 134.8 (xylyl Ar CH C3/6), 130.7 and 134.3 (xylyl Ar CH C4/5), 131.3 and 133.7 (xylyl Ar C C1/2), 137.6 (NCHN), 149.2 (benzimidazolium C−O), and 150.5 (benzimidazolium C−O).

4,7-Dibutoxybenzimidazole (16). Palladium on carbon (10%, 0.4 g) was added to a mixture of crude 1,4-dibutoxy-2,3-dinitrobenzene (6.6 g of mixture, ca. 17 mmol of 1,4-dibutoxy-2,3-dinitrobenzene) and ammonium formate (24 g, 0.38 mol) in water (40 mL) and ethanol (180 mL). The mixture was heated at ca. 60 °C for 1.25 h with stirring under a nitrogen atmosphere. The mixture was allowed to cool and was then filtered through Celite under nitrogen. The filtrate was concentrated in vacuo. The residue was treated with formic acid (90%, 66 mL), and the resulting mixture was heated at reflux for 2 h. The mixture was then allowed to cool overnight and was then filtered (byproduct crystallize/precipitate with slow cooling). The filter cake was washed with formic acid (90%, 20 mL). The formic acid solutions were combined and then treated with aqueous ammonia (28%, 200 mL). The resulting solid was collected and recrystallized from ethyl acetate (including treatment with activated carbon) to afford off-white crystals (2.5 g, 56%). $C_{15}H_{22}N_2O_2$ requires C, 68.67; H, 8.45; N, 10.68%. Found: C, 68.43; H, 8.17; N, 10.56; δ_H [$(CD_3)_2SO$, 300.1 MHz] 0.94 (6H, t, $^3J_{H,H}$ 7.4 Hz, 2 × CH_3), 1.48 (4H, m, 2 × CH_2CH_3), 1.73 (4H, m, 2 × OCH_2CH_2), 4.05 (2H, t, $^3J_{H,H}$ 6 Hz, OCH_2), 4.12 (2H, t, $^3J_{H,H}$ 6 Hz, OCH_2), 6.51 (1H, d,$^3J_{H,H}$ 8 Hz, Ar H), 6.59 (1H, d,$^3J_{H,H}$ 8 Hz, Ar H), 8.00 (1H, s, NCHN), and 12.62 (1H, s, NH); δ_C [$(CD_3)_2SO$, 75.5 MHz] 13.8 (CH_3), 18.76, 18.81 (2 × CH_2), 31.0, 31.1 (2 × CH_2), 67.8, 68.2 (2 × OCH_2), 103.9 (2 × Ar CH), 125.1 (Ar C), 135.0 (Ar C), 139.98 (Ar C), 140.01 (NCHN), and 144.7 (Ar C).

1,2-Bis(4′,7′-dibutoxybenzimidazolyl-1′-methyl)benzene (17). Sodium hydride (0.52 g, 13 mmol; 60% dispersion in oil) was added to a mixture of 4,7-dibutoxybenzimidazole (**16**) (2.49 g, 9.5 mmol) in dry THF (120 mL). The mixture was stirred for 40 min. To the resulting solution was added a solution of 1,2-bis(bromomethyl)-benzene (1.39 g, 5.25 mmol) in dry THF (45 mL). The mixture was then heated at reflux overnight. The mixture was cooled and then filtered through a plug of Celite. The filtrate was concentrated in vacuo; the residue was dissolved in ethyl acetate (150 mL), and the solution was filtered through a plug of silica. The filtrate was concentrated in vacuo, and the residue was triturated with hot hexanes (175 mL). The mixture was cooled; the solution was decanted, and the solid was triturated again with hot fresh hexanes (50 mL). After cooling, the solid was collected and recrystallized by dissolving the solid in dichloromethane (5 mL) and layering the solution with hexanes (100 mL), which afforded off-white crystals (2.12 g, 71%). $C_{38}H_{50}N_4O_4$ requires C, 72.81; H, 8.04; N, 8.94%. Found: C, 72.65; H, 7.90; N, 8.74; δ_H [$(CD_3)_2SO$, 500.1 MHz] 0.74 (6H, t, $^3J_{H,H}$ 7.4 Hz, 2 × CH_3), 0.95 (6H, t, $^3J_{H,H}$ 7.4 Hz, 2 × CH_3), 1.08−1.16 (4H, m, 2 × CH_2CH_3), 1.41−1.52 (8H, 2 × m, 2 × OCH_2CH_2 and 2 × CH_2CH_3), 1.71−1.76 (4H, m, 2 × OCH_2CH_2), 3.88 (4H, t, $^3J_{H,H}$ 6.5 Hz, 2 × OCH_2), 4.12 (4H, t, $^3J_{H,H}$ 6.5 Hz, 2 × OCH_2), 5.75 (4H, s, 2 × benzylic CH_2), 6.58 (2H, d, $^3J_{H,H}$ 8.6 Hz, 2 × benzimidazole Ar 7′-CH), 6.63 (2H, d, $^3J_{H,H}$ 8.6 Hz, 2 × benzimidazole Ar 6′-CH), 6.67−6.71 (2H, AA′ part of AA′XX′ pattern, xylyl Ar 3-CH and 6-CH), 7.16−7.20 (2H, XX′ part of AA′XX′ pattern, xylyl Ar 4-CH and 5-CH), and 7.95 (2H, s, 2 × NCHN); δ_C [$(CD_3)_2SO$, 125.8 MHz] 13.6 (CH_3), 13.8 (CH_3), 18.5 (CH_2CH_3), 18.8 (CH_2CH_3), 30.5 (OCH_2CH_2), 31.1 (OCH_2CH_2), 46.5 (benzylic CH_2), 67.9 (OCH_2), 68.2 (OCH_2), 104.3 (benzimidazole 5′-CH), 104.4 (benzimidazole 6′-CH), 124.9 (benzimidazole 8′-C), 126.4 (xylyl Ar 3-CH and 6-CH), 127.7 (xylyl Ar 4-CH and 5-CH), 135.1 (xylyl Ar 1-C and 2-C), 135.7 (benzimidazole 9′-C), 140.6 (benzimidazole B-CO), 143.0 (NCHN), and 144.8 (benzimidazole A-CO).

1,1′,3,3′-Bis(*o*-xylyl)bis(4′,7′-dibutoxybenzimidazolium)dibromide 12·2Br. Solutions of 1,2-bis(4′,7′-dibutoxybenzimidazolylmethyl)benzene (**17**) (1.44 g, 2.3 mmol) in acetone (60 mL) and 1,2-bis(bromomethyl)benzene (0.67 g, 2.5 mmol) in acetonitrile (60 mL) were added portionwise, simultaneously, to acetonitrile (500 mL) heated at reflux over the course of 6.5 h. The mixture was then heated at reflux overnight. The mixture was concentrated in vacuo. The residue was recrystallized by dissolving the solid in chloroform (8 mL) and layering the solution with ethyl acetate (110 mL), which afforded colorless crystals (1.72 g, 84%). $C_{46}H_{58}N_4O_4Br_2\cdot 3H_2O$ requires C, 58.48; H, 6.83; N, 5.93%. Found: C, 58.65; H, 6.63; N, 5.66; δ_C ($CDCl_3$, 125.8 MHz) 13.9 (CH_3), 19.3 (CH_2CH_3), 31.3 (OCH_2CH_2), 51.2 (benzylic CH_2), 70.1 (OCH_2), 109.0 (benzimidazolium 5′-CH and 6′-CH), 121.8 (benzimidazolium C), 131.4 (xylyl 1-C and 2-C), 131.9 (xylyl 4-C and 5-C), 134.8 (xylyl 3-C and 5-C), 140.3 (NCHN), and 141.3 (benzimidazolium C−O).

Structure Determinations. Full spheres of "low"-temperature CCD area detector diffractometer data were measured (Bruker AXS instrument, ω-scans; monochromatic Mo Kα radiation; $\lambda = 0.7107_3$ Å), yielding $N_{t(otal)}$ reflections, these merging to N unique (R_{int} cited) after "empirical"/multiscan absorption correction (proprietary software), N_o with $F > 4\sigma(F)$ being considered "observed" and used in the full matrix least-squares refinements on F^2; anisotropic displacement parameter forms were refined for the non-hydrogen atoms, hydrogen atom treatment following a "riding" model. Neutral atom complex scattering factors were employed within the Xtal 3.7 and SHELXL97 programs;[29] individual variations in procedure are noted as "variata". Pertinent results are given below and in the text and figures and the Supporting Information; full.cif depositions (excluding structure factor amplitudes) are deposited with the Cambridge Crystallographic Data Centre, CCDC 653544−653546.

8·2BPh$_4$: $C_{98}H_{118}B_2N_4$, $M_r = 1373.7$; triclinic, space group $P\bar{1}$, $a = 10.212(2)$, $b = 10.986(2)$, $c = 19.149(3)$ Å, $\alpha = 73.713(2)$, β

= 80.078(3), γ = 78.970(3)°, V = 2008 Å^3; D_c (Z = 1) = 1.13$_6$ g cm^{-3}; μ_{Mo} = 0.06 mm^{-1}; specimen: 0.65 × 0.08 × 0.02 mm; $T_{min/max}$ = 0.84; $2\theta_{max}$ = 58°; N_t = 20164, N = 9877 (R_{int} = 0.039), N_o = 5532; R = 0.049, R_w = 0.040; T ca. 153 K.

Variata. All hydrogen atoms were refined in $(x,y,z,U_{iso})_H$ (refinement on |F|).

11·2Br·5H$_2$O: $C_{46}H_{68}Br_2N_4O_7$, M_r = 980.9; triclinic, space group $P\bar{1}$, a = 9.051(2), b = 10.069(2), c = 27.751(5) Å, α = 80.531(3), β = 80.729(3), γ = 80.473(3)°, V = 2437 Å^3; D_c (Z = 2) = 1.33$_7$ g cm^{-3}; μ_{Mo} = 1.7 mm^{-1}; specimen: 0.68 × 0.08 × 0.06 mm; $T_{min/max}$ = 0.88; $2\theta_{max}$ = 50°; N_t = 23127, N = 8540 (R_{int} = 0.087), N_o = 6244; R = 0.056, R_w = 0.12; T ca. 153 K.

12·2Br·4H$_2$O: $C_{46}H_{66}Br_2N_4O_8$, M_r = 962.9; monoclinic, space group $C2/c$, a = 20.524(2), b = 20.512(2), c = 13.607(1) Å, β = 126.334(1)°, V = 4615 Å^3; D_c (Z = 4) = 1.38$_6$ g cm^{-3}; μ_{Mo} = 1.8 mm^{-1}; specimen: 0.55 × 0.38 × 0.24 mm; $T_{min/max}$ = 0.74; $2\theta_{max}$ = 66°; N_t = 31846, N = 8619 (R_{int} = 0.023), N_o = 6926; R = 0.034, R_w = 0.063; T ca. 170 K.

Variata. Hydrolytic hydrogen atoms were refined in (x,y,z,U_{iso}).

Acknowledgment. We thank the Australian Research Council for a Discovery Grant (to M.V.B. and A.H.W.) and an Australian Postgraduate Award (to C.C.W.), the School of Biomedical, Biomolecular and Chemical Sciences (UWA) for a summer vacation scholarship (to C.H.H.), and Curtin University of Technology for a Research and Teaching Fellowship (to D.H.B.).

Supporting Information Available: Tables of ^{1}H NMR data and ^{1}H NMR spectra for the cyclophane salts **8**·2Br, **8**·2PF$_6$, **9**·2Br, **10**·2Br, **11**·2Br, and **12**·2Br in various solvents including DMSO-d_6, CD_3OD, CH_3OH, CD_2Cl_2, and $CDCl_3$; Job plot information for **8**; details about the estimation of rate constants and activation energies for dynamic NMR experiments; ^{13}C NMR spectra for **8**·2Br, **11**·2Br, and **12**·2Br; ^{1}H and ^{13}C NMR spectra for **14**, **15**, **16**, and **17**; tables detailing the hydrogen bonding in the solid-state structures of **11**·2Br and **12**·2Br; figures of the unit cells and hydrogen bonding for **11**·2Br·5H$_2$O and **12**·2Br·4H$_2$O; and figures containing atom labels for the solid-state structures of cations **8**, **11**, and **12**. This material is available free of charge via the Internet at http://pubs.acs.org.

JO801860D

(29) (a) Hall, S. R., du Boulay, D. J., Olthof-Hazekamp, R., Eds. *The Xtal 3.7 System*; The University of Western Australia: Perth, Australia, 2001. (b) Sheldrick, G. M. *SHELXL-97. A Program for Crystal Structure Refinement*; University of Göttingen: Göttingen, Germany, 1997.